Control of Ligand Field Strength through Intra- and Interligand Contact. Octahedral Iron(II) Poly(pyrazolyl)borate Complexes

Yoshiki Sohrin,*,† Hisao Kokusen,‡ and Masakazu Matsui†

Institute for Chemical Research, Kyoto University, Uji, Kyoto 611, Japan, and Faculty of Education, Tokyo Gakugei University, Koganei, Tokyo 184, Japan

Received February 17, 1995⊗

The spin state of Fe(II) poly(pyrazolyl)borate complexes is highly dependent upon substituents on the ligand molecule. While $[B(pz)_4]_2Fe$ (**1**, pz = 1-pyrazolyl) and $[PhB(pz)_3]_2Fe$ (**2**) are in a low-spin state in $CHCl_3$ at ambient temperature, $[HB(pz)_3]_2Fe$ (**3**) is in a spin-crossover state and $[HB(3,5\text{-}Me_2pz)_3]_2Fe$ (**4**) is in a high-spin state. Here, we present the first rational explanation of spin-crossover caused by substituents. X-ray structures of low-spin **1** (the triclinic space group $P\bar{1}$ with a = 11.943(3) Å, b = 12.310(3) Å, c = 9.628(2) Å, α = 96.12(2)°, β = 101.22(1)°, γ = 100.02(2)°, V = 1352.7(5) Å^3, and Z = 2) and **2** (the orthorhombic space group $Pca2_1$ with a = 18.046(2) Å, b = 8.894(3) Å, c = 18.309(4) Å, V = 2938(1) Å^3, and Z = 4) were determined and compared with the reported structures of low-spin **3** and high-spin **4**. All the complexes had a trigonally distorted geometry, and the ligands were tridentate. ^{1}H-NMR suggested that the solution structures of the complexes were similar to the X-ray structures. The key to the issue was the size of the Fe(II) ion. The fourth substituents on the boron atom in **1** and **2** forced a narrow arrangement on the tripod of the coordinated pyrazolyl groups and favored low-spin complex formation with a small Fe(II) ion. For **4**, the methyl group at the 3-position of the pyrazolyl ring brought about severe interligand contact around the metal ion and prohibited low-spin complex formation. These contacts were ascertained by means of molecular mechanics calculations. Consequently, poly(pyrazolyl)borates can control the electron configuration of Fe(II) ion through intra- and interligand contact.

Introduction

Poly(pyrazolyl)borate complexes have various unique characteristics.[1] The spin state of poly(pyrazolyl)borate Fe(II) complexes is an intriguing subject. Tris- and tetrakis(pyrazolyl)borates (A^-) are tridentate ligands and form octahedral A_2Fe complexes. $[B(pz)_4]_2Fe$ (**1**) and $[PhB(pz)_3]_2Fe$ (**2**) in $CHCl_3$ are low-spin at 240−330 K (pz = 1-pyrazolyl).[2] The magnetic dipole moment of $[HB(pz)_3]_2Fe$ (**3**) is 2.7 μ_B in CH_2Cl_2 at room temperature and increases with an increase in temperature. On the other hand, $[HB(3,5\text{-}Me_2pz)_3]_2Fe$ (**4**) and $[HB(3,4,5\text{-}Me_3pz)_3]_2Fe$ (**5**) are fully paramagnetic high-spin compounds in $CHCl_3$ (5.0 and 5.2 μ_B, respectively). Although the drastic dependence of ligand field strength upon substituents has been known since 1967, immediately after the first synthesis of poly(pyrazolyl)borates, the origin of this dependence has not been elucidated.

Many investigators studied the spin state of poly(pyrazolyl)borate Fe(II) complexes. Beattie et al. have reported that the partial molar volume of **3** in tetrahydrofuran increases by 22 cm^3 mol^{-1} when **3** is taken from a low-spin to a high-spin state.[3] The volume change probably corresponds to a 0.10−0.15 Å change in the Fe−N bond length. In the solid state, **1** and **3** are normally low-spin, whereas **4** and **5** are high-spin.[4] The low-spin **3** complex undergoes spin crossover to the high-spin state under high temperature or pressure. Compounds **4** and **5** are converted to the low-spin state under conditions of low temperature or high pressure. Gas-phase ultraviolet photoelectron studies have shown that **3** has a high-spin $^5T_{2g}$ ground-state configuration at 400 K.[5] Recently, the first high-spin state of **1** was found in the gas phase of a 480−560 K temperature range.[6] These results indicate that the ligands substituted on the 3-position of the pyrazolyl group prefer the high-spin state and that ligands having a fourth ring on the boron atom prefer the low-spin state. Hutchinson et al. have revealed the X-ray structures of low-spin **3** and high-spin **4**.[7] We determined the crystal structures of low-spin **1** and **2**. From these structures, we realized that the steric effects of substituents, namely intra- and interligand contact, are crucial for electron configuration of the Fe(II) poly(pyrazolyl)borate complexes. Moreover, we estimated the strain energy change accompanying the complex formation by a simple molecular mechanics (MM) calculation and substantiated the steric effect.

* Author to whom correspondence should be addressed.
† Kyoto University.
‡ Tokyo Gakugei University.
⊗ Abstract published in *Advance ACS Abstracts,* June 15, 1995.

(1) (a) Trofimenko, S. *Chem. Rev.* **1972**, *72*, 497−509. (b) Trofimenko, S. *Prog. Inorg. Chem.* **1986**, *34*, 115−210. (c) Trofimenko, S. *Chem. Rev.* **1993**, *93*, 943−980.
(2) Jesson, J. P.; Trofimenko, S.; Eaton, D. R. *J. Am. Chem. Soc.* **1967**, *89*, 3158−3164. μ_B of **3** was measured in CH_2Cl_2 because of solubility. All others were measured in $CHCl_3$. Judging from the data of refs 2−7, the trends in μ_B should be not solvent dependent, when a specific interaction is not present between the complex and solvent molecules.
(3) (a) Beattie, J. K.; Binstead, R. A.; West, R. J. *J. Am. Chem. Soc.* **1978**, *100*, 3044−3050. (b) Binstead, R. A.; Beattie, J. K. *Inorg. Chem.* **1986**, *25*, 1481−1484.
(4) (a) Jesson, J. P.; Weiher, J. F. *J. Chem. Phys.* **1967**, *46*, 1995−1996. (b) Jesson, J. P.; Weiher, J. F.; Trofimenko, S. *J. Chem. Phys.* **1968**, *48*, 2058−2066. (c) Hutchinson, B.; Daniels, L.; Henderson, E.; Neill, P.; Long, G. J.; Becker, L. W. *J. Chem. Soc., Chem. Commun.* **1979**, 1003−1005. (d) Long, G. J.; Hutchinson, B. B. *Inorg. Chem.* **1987**, *26*, 608−613. (e) Grandjean, F.; Long, G. J.; Hutchinson, B. B.; Ohlhausen, L.; Neill, P.; Holcomb, J. D. *Inorg. Chem.* **1989**, *28*, 4406−4414.
(5) Bruno, G.; Centineo, G.; Ciliberto, E.; Di Bella, S.; Fragalà, I. *Inorg. Chem.* **1984**, *23*, 1832−1836.
(6) Gulino, A.; Ciliberto, E.; Di Bella, S.; Fragalà, I. *Inorg. Chem.* **1993**, *32*, 3759−3761.
(7) Oliver, J. D.; Mullica, D. F.; Hutchinson, B. B.; Milligan, W. O. *Inorg. Chem.* **1980**, *19*, 165−169.

0020-1669/95/1334-3928$09.00/0

Table 1. Crystallographic Data

$[B(pz)_4]_2Fe$ (**1**)	
$C_{24}H_{24}N_{16}B_2Fe$	fw = 614.03
a = 11.943(3) Å	triclinic $P\bar{1}$ (No. 2)
b = 12.310(3) Å	T = 20 °C
c = 9.628(2) Å	λ = 1.541 78 Å
α = 96.12(2)°	ϱ_{calcd} = 1.507 g cm^{-3}
β = 101.22(1)°	μ = 48.83 cm^{-1}
γ = 100.02(2)°	$R(F_o)^a$ = 0.043
V = 1352.7(5) Å^3	$R_w(F_o)^b$ = 0.051
Z = 2	goodness of fit = 1.38
rflns collcd = 3787	indep rflns obsd = 2385
indep rflns = 3592	
$[PhB(pz)_3]_2Fe$ (**2**)	
$C_{30}H_{28}N_{12}B_2Fe$	fw = 634.10
a = 18.046(2) Å	orthorhombic $Pca2_1$ (No. 29)
b = 8.894(3) Å	T = 20 °C
c = 18.309(4) Å	λ = 1.541 78 Å
V = 2938(1) Å^3	ϱ_{calcd} = 1.433 g cm^{-3}
Z = 4	μ = 44.75 cm^{-1}
rflns collcd = 2337	$R(F_o)^a$ = 0.058
indep rflns obsd = 1930	$R_w(F_o)^b$ = 0.084
goodness of fit = 2.17	

$^a R = \sum(||F_o| - |F_c||)/\sum|F_o|$. $^b R_w = [\sum w(|F_o| - |F_c|)^2/\sum w|F_o|^2]^{1/2}$.

Experimental Section

General Procedures. $K[B(pz)_4]$ was synthesized as reported.[8] All other chemicals were reagent-grade, and distilled water was used throughout. Proton NMR spectra were obtained at 25 ± 1 °C using a Varian VXR 200 spectrometer. Chemical shifts are reported (ppm) downfield from TMS using the solvents $CDCl_3$ (δ_H = 7.25 ppm) as an internal standard. The reported ^1H coupling constants are $^3J_{HH}$ values.

Bis[tetrakis(pyrazolyl)borato]iron(II), $[B(pz)_4]_2Fe$ (1). Forty milliliters of 0.05 M sodium hydroxide containing $K[B(pz)_4]$ (0.64 g, 2.0 mmol) was added to 1 M hydrochloric acid (10 mL) containing $FeSO_4(NH_4)_2SO_4{\cdot}6H_2O$ (0.39 g, 1.0 mmol). Sodium hydroxide (1 M) was added and mixed until a reddish brown precipitate no longer formed (pH 1.2). After 20 min, the precipitate was filtered off and then washed with distilled water and methanol. Crystals for the analytical sample and the X-ray structure were obtained by recrystallization from chloroform. Anal. Calcd for $C_{24}H_{24}N_{16}B_2Fe$: C, 46.94; H, 3.94; N, 36.50. Found C, 46.12; H, 3.88; N, 35.98. ^1H NMR ($CDCl_3$, δ): 5.83 (3; br); 6.04 (3; br); 6.79 (1; br); 7.67 (3; br); 8.15 (1; br); 8.49 (1; br).

Tetrabutylammonium Phenyltris(pyrazolyl)borate. $[PhB(pz)_3]^-$ was synthesized according to the procedure of Trofimenko.[9] Pyrazole (25 g, 0.37 mol) and phenyldichloroborane (5.0 g, 0.03 mol) formed a precipitate of $[H_2pz]^+[PhB(pz)_3]^-$ in anhydrous toluene. The precipitate was filtered and washed with ether. A 3 mmol (1.1 g) amount of $[H_2pz]^+[PhB(pz)_3]^-$ was dissolved in 50 mL of 0.1 M sodium hydroxide. To this solution 1.9 g (6 mmol) of tetrabutylammonium bromide was added. The resulting white precipitate was filtered off, washed with water, and air dried. Anal. Calcd for $C_{31}H_{50}N_7B$: C, 70.04; H, 9.48; N, 18.45. Found C, 69.37; H, 9.56; N, 18.30.

Bis[phenyltris(pyrazolyl)borato]iron(II), $[PhB(pz)_3]_2Fe$ (2). Ten milliliters of 0.1 M sodium hydroxide containing $[N(Bu)_4]^+[PhB(pz)_3]^-$ (1.1 g, 2.0 mmol) was added to 0.1 M hydrochloric acid (20 mL) containing $FeSO_4(NH_4)_2SO_4{\cdot}6H_2O$ (0.39 g, 1.0 mmol). Sodium hydroxide (1 M) was added and mixed until a reddish brown precipitate no longer formed (pH 2.7). After 20 min, the precipitate was filtered off and then washed with distilled water and methanol. Crystals for the analytical sample and the X-ray structure were obtained by recrystallization from chloroform. Anal. Calcd for $C_{30}H_{28}N_{12}B_2Fe$: C, 56.82; H, 4.45; N, 26.51. Found C, 56.70; H, 4.37; N, 26.69. ^1H NMR ($CDCl_3$, δ): 6.17 (6; br, pz); 6.79 (6; br, pz); 7.60 (6; mult, Ph(3,4,5)); 7.82 (6; br, pz); 8.24 (4; d, J = 6.6 Hz, Ph(2,6)).

X-ray Crystal Structure Determination. Crystallographic data are summarized in Table 1. Crystals of **1** and **2** were mounted onto fine glass fibers with epoxy cement. The lattice parameters and intensity data were measured on a Rigaku AFC7R four-circle diffractometer with Ni-filtered Cu Kα radiation (λ = 1.541 78 Å) at 20 ± 1 °C. An ω–2θ scan to a maximum 2θ value of 120° was used. An empirical absorption correction using the program DIFABS[10] was applied to the data sets. The data were corrected for Lorentz and polarization effects, and a correction for secondary extinction was applied to **2**. The structures were solved by direct methods[11] and expanded using Fourier technique.[12] The non-hydrogen atoms were refined anisotropically. Hydrogens were fixed at the positions generated by calculation. All calculations were performed using the teXsan crystallographic software package developed by Molecular Structure Corp.

Figures 1 and 2 show the ORTEP drawings of **1** and **2**, respectively. Tables 2 and 3 list the atomic coordinates of non-hydrogen atoms. Tables 4 and 5 contain selected bond distances and bond angles for **1** and **2**, respectively. The mean dimensions of chelate rings for the Fe(II) complexes are summarized in Table 6; the labeling of atoms is given in Chart 1.

Table 2. Refined Atomic Coordinates and B_{eq} Values (Å^2) for **1**

atom	x	y	z	$B_{eq}{}^a$
Fe(1)	0	0	0	3.22(3)
Fe(2)	0.5	0.5	0.5	3.38(3)
N(1)	0.0312(4)	0.0944(4)	−0.1474(4)	3.6(1)
N(2)	0.1045(4)	0.0691(4)	−0.2344(4)	3.5(1)
N(3)	0.1673(4)	−0.0050(4)	0.0429(5)	3.7(1)
N(4)	0.2251(4)	−0.0246(3)	−0.0656(4)	3.5(1)
N(5)	−0.0273(4)	−0.1300(4)	−0.1431(4)	3.4(1)
N(6)	0.0459(3)	−0.1354(4)	−0.2365(4)	3.4(1)
N(7)	0.3127(4)	−0.1129(4)	−0.3066(5)	4.5(1)
N(8)	0.2175(4)	−0.0651(4)	−0.3347(4)	3.5(1)
N(9)	0.4692(4)	0.3538(4)	0.5675(5)	3.8(1)
N(10)	0.5497(4)	0.3265(4)	0.6744(5)	3.7(1)
N(11)	0.6610(4)	0.4785(4)	0.5048(5)	3.8(1)
N(12)	0.7233(4)	0.4400(4)	0.6169(4)	3.6(1)
N(13)	0.5510(4)	0.5706(4)	0.7009(4)	3.7(1)
N(14)	0.6234(4)	0.5245(4)	0.7939(4)	3.7(1)
N(15)	0.8508(5)	0.4198(5)	0.9041(6)	6.1(2)
N(16)	0.7347(4)	0.3793(4)	0.8646(5)	4.4(1)
C(1)	0.0134(5)	0.1951(5)	−0.1674(6)	3.9(1)
C(2)	0.0751(5)	0.2384(5)	−0.2648(6)	4.6(2)
C(3)	0.1319(5)	0.1571(5)	−0.3042(6)	4.0(1)
C(4)	0.2479(5)	0.0177(5)	0.1626(6)	4.0(1)
C(5)	0.3585(5)	0.0149(5)	0.1372(6)	4.3(1)
C(6)	0.3406(5)	−0.0112(5)	−0.0068(6)	4.2(1)
C(7)	−0.1095(5)	−0.2223(5)	−0.1828(6)	3.8(1)
C(8)	−0.0922(5)	−0.2884(5)	−0.3002(6)	4.2(1)
C(9)	0.0077(5)	−0.2307(5)	−0.3313(5)	3.9(1)
C(10)	0.3304(5)	−0.1473(5)	−0.4354(6)	4.9(2)
C(11)	0.2493(5)	−0.1254(5)	−0.5437(6)	4.4(2)
C(12)	0.1777(5)	−0.0723(5)	−0.4784(6)	4.0(1)
C(13)	0.3887(5)	0.2622(5)	0.5208(6)	4.3(1)
C(14)	0.4140(5)	0.1740(5)	0.5921(7)	4.8(2)
C(15)	0.5162(5)	0.2189(5)	0.6893(6)	4.3(2)
C(16)	0.7280(5)	0.4875(5)	0.4088(6)	3.8(1)
C(17)	0.8307(5)	0.4521(5)	0.4567(6)	4.0(1)
C(18)	0.8251(4)	0.4233(4)	0.5879(6)	3.8(1)
C(19)	0.5344(5)	0.6621(5)	0.7773(7)	4.6(2)
C(20)	0.5968(5)	0.6753(5)	0.9180(6)	4.9(2)
C(21)	0.6507(5)	0.5865(5)	0.9245(6)	4.6(2)
C(22)	0.8838(6)	0.3926(7)	1.0353(7)	6.3(2)
C(23)	0.7903(7)	0.3349(6)	1.0795(7)	6.1(2)
C(24)	0.6980(6)	0.3289(6)	0.9715(7)	5.9(2)
B(1)	0.1520(5)	−0.0392(5)	−0.2190(6)	3.6(2)
B(2)	0.6593(6)	0.4161(6)	0.7396(7)	3.9(2)

$^a B_{eq} = 8\pi^2(U_{11}(aa^*)^2 + U_{22}(bb^*)^2 + U_{33}(cc^*)^2 + 2U_{12}aa^*bb^* \cos\gamma + 2U_{13}aa^*cc^* \cos\beta + 2U_{23}bb^*cc^* \cos\alpha)/3$.

(8) Trofimenko, S. *J. Am. Chem. Soc.* **1967**, *89*, 3170–3177.
(9) Trofimenko, S. *J. Am. Chem. Soc.* **1967**, *89*, 6288–6294.
(10) Walker, N; Stuart, D. *Acta Crystallogr., Sect. A* **1983**, *39*, 158–166.
(11) Sheldrick, G. M. In *Crystallographic Computing*; Sheldrick, G. M., Kruger C., Goddard, R., Eds.; Oxford University Press: Oxford, England, 1985; Vol. 3, pp 175–189.
(12) Beurskens, P. T.; Admiraal, G.; Beurskens, G.; Bosman, W. P.; Garcia-Granda, S.; Gould, R. O.; Smits, J. M. M.; Smykalla, C. *The DIRDIF program system, Technical Report of the Crystallography Laboratory*; University of Nijmegen: Nijmegen, The Netherlands, 1992.

Table 3. Refined Atomic Coordinates and B_{eq} Values (Å^2) for **2**

atom	x	y	z	B_{eq}[a]
Fe(1)	0.93253(7)	0.3401(1)	0.2471	2.40(3)
N(1)	0.8343(5)	0.2917(8)	0.2745(5)	2.8(2)
N(2)	0.7973(4)	0.3904(8)	0.3168(5)	2.7(2)
N(3)	0.9559(4)	0.4241(8)	0.3352(5)	2.7(2)
N(4)	0.9083(4)	0.5157(8)	0.3722(4)	2.6(2)
N(5)	0.8945(4)	0.5399(8)	0.2114(5)	2.6(2)
N(6)	0.8523(4)	0.6222(8)	0.2606(5)	2.8(2)
N(7)	1.0329(4)	0.3888(8)	0.2018(5)	2.6(2)
N(8)	1.0751(4)	0.2827(9)	0.1651(5)	3.0(2)
N(9)	0.9109(4)	0.2561(8)	0.1420(5)	2.7(2)
N(10)	0.9628(4)	0.1686(8)	0.1081(5)	2.8(2)
N(11)	0.9723(4)	0.1393(9)	0.2671(4)	2.8(2)
N(12)	1.0181(4)	0.0632(7)	0.2220(5)	2.7(2)
C(1)	0.7922(6)	0.1665(9)	0.2695(6)	3.3(3)
C(2)	0.7263(6)	0.189(1)	0.3080(7)	3.9(3)
C(3)	0.7310(5)	0.329(1)	0.3364(7)	3.2(2)
C(4)	1.0188(5)	0.430(1)	0.3734(6)	3.3(2)
C(5)	1.0133(6)	0.522(1)	0.4333(6)	3.7(3)
C(6)	0.9419(5)	0.576(1)	0.4310(6)	3.1(2)
C(7)	0.9099(6)	0.635(1)	0.1576(6)	3.3(2)
C(8)	0.8812(7)	0.778(1)	0.1707(7)	3.7(3)
C(9)	0.8457(5)	0.7663(10)	0.2360(7)	3.0(2)
C(10)	0.7733(5)	0.634(1)	0.3858(6)	2.7(2)
C(11)	0.7681(5)	0.597(1)	0.4584(7)	3.2(2)
C(12)	0.7143(6)	0.661(1)	0.5048(6)	3.8(3)
C(13)	0.6648(7)	0.762(2)	0.4756(8)	4.9(3)
C(14)	0.6687(5)	0.801(1)	0.4025(8)	4.2(3)
C(15)	0.7208(5)	0.738(1)	0.3576(7)	3.3(2)
C(16)	1.0784(5)	0.508(1)	0.2146(7)	3.7(2)
C(17)	1.1493(6)	0.476(1)	0.1889(7)	4.3(3)
C(18)	1.1449(5)	0.336(1)	0.1574(7)	4.0(3)
C(19)	0.8525(6)	0.265(1)	0.0957(7)	3.7(3)
C(20)	0.8666(6)	0.185(1)	0.0343(7)	4.2(3)
C(21)	0.9368(6)	0.127(1)	0.0438(7)	3.7(3)
C(22)	0.9660(6)	0.063(1)	0.3286(6)	3.2(2)
C(23)	1.0111(5)	−0.065(1)	0.3254(6)	3.2(2)
C(24)	1.0415(6)	−0.058(1)	0.2586(5)	2.9(2)
C(25)	1.0833(5)	0.021(1)	0.0936(6)	2.8(2)
C(26)	1.1337(6)	0.074(1)	0.0407(7)	4.1(3)
C(27)	1.1659(6)	−0.023(1)	−0.0084(7)	4.1(3)
C(28)	1.1501(6)	−0.173(1)	−0.0076(8)	4.2(3)
C(29)	1.1017(8)	−0.228(1)	0.0417(8)	4.8(3)
C(30)	1.0688(6)	−0.134(1)	0.0906(7)	3.8(3)
B(1)	0.8307(6)	0.546(1)	0.3354(6)	2.5(2)
B(2)	1.0364(6)	0.130(1)	0.1450(8)	3.0(3)

[a] $B_{eq} = 8\pi^2(U_{11}(aa^*)^2 + U_{22}(bb^*)^2 + U_{33}(cc^*)^2 + 2U_{12}aa^*bb^* \cos\gamma + 2U_{13}aa^*cc^* \cos\beta + 2U_{23}bb^*cc^* \cos\alpha)/3$.

Molecular Mechanics Calculations. These were carried out using a CAChe system (version 3.5, CAChe Scientific) on a Macintosh Quadra 800. The program based on Allinger's MM2 force field[13] computed the net force acting on a molecule as the sum of the energy in terms of bond stretch, bond angle, dihedral angle, improper torsion, van der Waals, electrostatics, and hydrogen bond. The augmented force field parameters by CAChe were used for low-spin Fe(II) complexes, of which the ideal length (r_0) of the Fe−N bond was 1.926 Å. To calculate the high-spin Fe(II) complexes, r_0 of the Fe−N bond was assumed to be 2.130 Å. The other parameters, such as the Fe−N force constant, were not changed, since they had minor effects on the calculated dimensions of complexes. Charges of −1 and +2 were assigned to boron and iron(II) atoms, respectively. Fe−N bonds were described as coordinate bonds. Under these conditions, pyrazole rings were treated as aromatic.

The X-ray structure was used as the initial conformation for calculation of the complex. The high-spin models of **1**−**3** were deduced from the X-ray structure of **4**, and low-spin **4** was modeled on the basis of the X-ray structure of **3**. The geometry was optimized with locking the intraligand N···N distances (bite sizes). Locking assigned a large force constant and set the geometry to a given value. This locking was necessary to prevent the bite sizes from becoming smaller especially for high-spin models. However, the presence and absence of the locking had only a minor effect on the steric energy of the optimized geometry.

(13) (a) Allinger, N. L. *J. Am. Chem. Soc.* **1977**, *99*, 8127−8134. (b) Burkert, U.; Allinger, N. L. *Molecular Mechanics*; The American Chemical Society: Washington, DC, 1982.

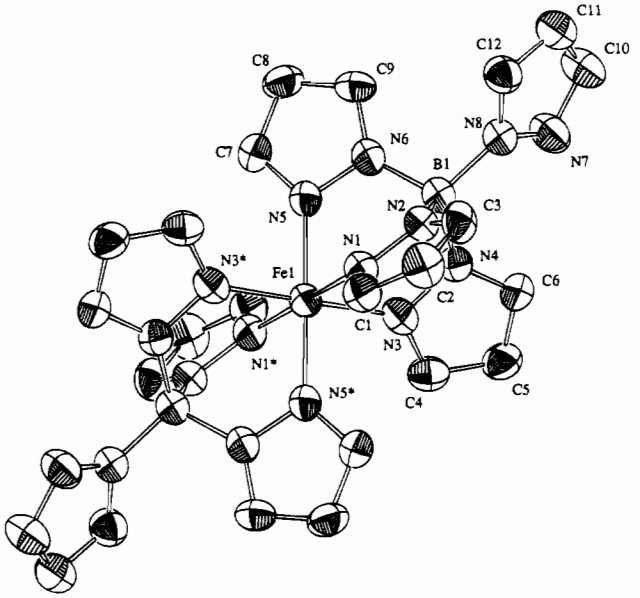

Figure 1. ORTEP view of one of the independent molecules of $[B(pz)_4]_2Fe$ (**1**) (50% probability). Hydrogen atoms are omitted for clarity.

Table 4. Selected Bond Distances (Å) and Bond Angles (deg) for $[B(pz)_4]_2Fe$ (**1**)

Molecule 1

Bond Distances

Fe(1)−N(1)	1.977(4)	Fe(1)−N(3)	1.973(4)
Fe(1)−N(5)	1.934(4)	N(1)−N(2)	1.374(5)
N(2)−B(1)	1.547(7)	N(3)−N(4)	1.382(5)
N(4)−B(1)	1.538(7)	N(5)−N(6)	1.375(5)
N(6)−B(1)	1.546(7)	N(7)−N(8)	1.363(5)
N(8)−B(1)	1.519(6)		

Bond Angles

N(1)−Fe(1)−N(1′)	180.0	N(1)−Fe(1)−N(3)	87.8(2)
N(1)−Fe(1)−N(5)	88.8(2)	N(3)−Fe(1)−N(3′)	180.0
N(3)−Fe(1)−N(5)	89.2(2)	N(5)−Fe(1)−N(5′)	180.0
Fe(1)−N(1)−N(2)	120.0(3)	N(1)−N(2)−B(1)	117.2(4)
Fe(1)−N(3)−N(4)	121.1(3)	N(3)−N(4)−B(1)	116.0(4)
Fe(1)−N(5)−N(6)	119.6(3)	N(5)−N(6)−B(1)	118.6(4)
N(7)−N(8)−B(1)	120.9(4)	N(2)−B(1)−N(4)	106.6(4)
N(2)−B(1)−N(6)	107.2(4)	N(2)−B(1)−N(8)	111.6(4)
N(4)−B(1)−N(6)	108.8(4)	N(4)−B(1)−N(8)	114.3(4)
N(6)−B(1)−N(8)	108.1(4)		

Molecule 2

Bond Distances

Fe(2)−N(9)	1.977(4)	Fe(2)−N(11)	1.978(4)
Fe(2)−N(13)	1.967(4)	N(9)−N(10)	1.377(6)
N(10)−B(2)	1.534(8)	N(11)−N(12)	1.364(5)
N(12)−B(2)	1.555(7)	N(13)−N(14)	1.360(6)
N(14)−B(2)	1.540(7)	N(15)−N(16)	1.353(6)
N(16)−B(2)	1.517(7)		

Bond Angles

N(9)−Fe(2)−N(9′)	180.0	N(9)−Fe(2)−N(11)	87.5(2)
N(9)−Fe(2)−N(13)	88.7(2)	N(11)−Fe(2)−N(11′)	180.0
N(11)−Fe(2)−N(13)	88.7(2)	N(13)−Fe(2)−N(13′)	180.0
Fe(2)−N(9)−N(10)	120.2(4)	N(9)−N(10)−B(2)	116.7(4)
Fe(2)−N(11)−N(12)	121.8(3)	N(11)−N(12)−B(2)	115.2(4)
Fe(2)−N(13)−N(14)	119.0(3)	N(13)−N(14)−B(2)	118.9(4)
N(15)−N(16)−B(2)	121.6(5)	N(10)−B(2)−N(12)	107.0(4)
N(10)−B(2)−N(14)	109.4(4)	N(10)−B(2)−N(16)	111.1(5)
N(12)−B(2)−N(14)	107.8(4)	N(12)−B(2)−N(16)	112.9(5)
N(14)−B(2)−N(16)	108.5(5)		

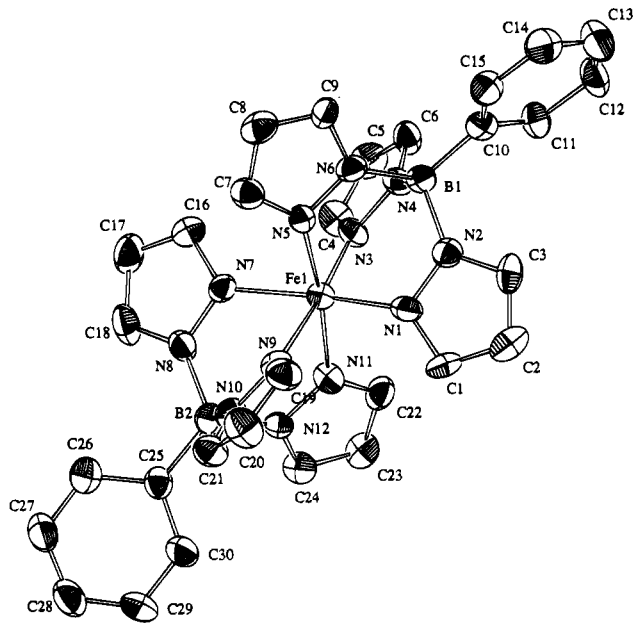

Figure 2. ORTEP view of $[PhB(pz)_3]_2Fe$ (**2**) (50% probability). Hydrogen atoms are omitted for clarity.

Results

Syntheses of Complexes. Complexes with two $[B(pz)_4]^-$ and $[PhB(pz)_3]^-$ ligands (A^-) coordinated to Fe(II) were produced according to the following equation:

$$Fe^{2+} + 2HA \rightleftharpoons A_2Fe + 2H^+ \quad (1)$$

The complexes were obtained as precipitates and dissolved into chloroform, dichloromethane, and benzene. These complexes were stable in air.

Structure of $[B(pz)_4]_2Fe$ (1). Two crystallographically independent molecules, lying on an inversion point in the crystal, were contained in a unit cell of complex **1**. These two molecules were similar. Figure 1 shows an ORTEP drawing of one of these molecules, Table 2 lists the atomic coordinates of non-hydrogen atoms, and Table 4 shows selected bond distances and angles. The molecule is monomeric with no short intermolecular contacts. The Fe(II) atom sits on a center of inversion. Both ligands are tridentate, and the geometry about the Fe(II) atom is a trigonally distorted octahedron. This structure is similar to that observed for $[HB(pz)_3]_2Fe$ (**3**),[7] while the noncoordinated pyrazolyl ring stands out in the direction opposite the metal atom.

Structure of $[PhB(pz)_3]_2Fe$ (2). Figure 2 shows an ORTEP drawing of **2**, Table 3 lists the atomic coordinates of non-hydrogen atoms, and Table 5 shows selected bond distances and angles. Both ligands are tridentate, forming a six-coordinated, monomeric structure. The structure of **2** basically resembles that of **1**. The fourth pyrazolyl ring in **1** is replaced with a phenyl ring in **2**. However, the octahedral geometry about the Fe(II) atom in **2** is more distorted than that in **1**. While the Fe–N bond length is 1.934–1.978 Å for **1**, it ranges between 1.828 and 2.102 Å for **2**. The N–Fe–N bond angles in chelate rings are 87.5–89.2° for **1** and 82.4–94.3 for **2**.

Molecular Mechanics Calculations. The global minimum in steric energy of free ligand ($U_{A^-,min}$) was 9.6 kcal/mol for $[B(pz)_4]^-$, 4.8 for $[PhB(pz)_3]^-$, 8.4 for $[HB(pz)_3]^-$, and −4.1 for $[HB(3,5\text{-}Me_2pz)_3]^-$.[14] The global minimum configuration of $[HB(pz)_3]^-$ and $[HB(3,5\text{-}Me_2pz)_3]^-$ resembled a propeller. The configuration of $[B(pz)_4]^-$ and $[PhB(pz)_3]^-$ was similar to that from the X-ray structure of $[B(pz)_4]^-$ in the crystals of sodium and potassium salts.[15] Two pyrazolyl groups formed a shallow V-wing. The third ring (pz or Ph) was oriented so as to bisect the wing, and the fourth ring was nearly perpendicular to the third ring. The energy barrier to rotation of pyrazolyl rings around the N–B bond was much higher for $[B(pz)_4]^-$ and $[PhB(pz)_3]^-$ than that for $[HB(pz)_3]^-$ and $[HB(3,5\text{-}Me_2pz)_3]^-$.

Table 5. Selected Bond Distances (Å) and Bond Angles (deg) for $[PhB(pz)_3]_2Fe$ (**2**)

Bond Distances			
Fe(1)–N(1)	1.892(8)	Fe(1)–N(3)	1.828(8)
Fe(1)–N(5)	2.014(7)	Fe(1)–N(7)	2.039(8)
Fe(1)–N(9)	2.102(9)	Fe(1)–N(11)	1.960(8)
N(1)–N(2)	1.35(1)	N(2)–B(1)	1.55(1)
N(3)–N(4)	1.36(1)	N(4)–B(1)	1.58(1)
N(5)–N(6)	1.39(1)	N(6)–B(1)	1.58(1)
N(7)–N(8)	1.39(1)	N(8)–B(2)	1.57(1)
N(9)–N(10)	1.37(1)	N(10)–B(2)	1.53(1)
N(11)–N(12)	1.35(1)	N(12)–B(2)	1.56(2)
C(10)–B(1)	1.59(1)	C(25)–B(2)	1.60(1)
Bond Angles			
N(1)–Fe(1)–N(3)	94.3(3)	N(1)–Fe(1)–N(5)	88.2(3)
N(1)–Fe(1)–N(7)	171.4(4)	N(1)–Fe(1)–N(9)	89.3(3)
N(1)–Fe(1)–N(11)	94.9(3)	N(3)–Fe(1)–N(5)	90.3(3)
N(3)–Fe(1)–N(7)	93.9(3)	N(3)–Fe(1)–N(9)	175.6(3)
N(3)–Fe(1)–N(11)	97.1(3)	N(5)–Fe(1)–N(7)	89.0(3)
N(5)–Fe(1)–N(9)	87.3(3)	N(5)–Fe(1)–N(11)	171.8(4)
N(7)–Fe(1)–N(9)	82.4(3)	N(7)–Fe(1)–N(11)	86.8(3)
N(9)–Fe(1)–N(11)	85.1(3)	Fe(1)–N(1)–N(2)	117.9(6)
N(1)–N(2)–B(1)	121.1(8)	Fe(1)–N(3)–N(4)	122.4(6)
N(3)–N(4)–B(1)	116.8(7)	Fe(1)–N(5)–N(6)	116.2(6)
N(5)–N(6)–B(1)	118.4(7)	Fe(1)–N(7)–N(8)	122.7(5)
N(7)–N(8)–B(2)	117.2(7)	Fe(1)–N(9)–N(10)	119.4(6)
N(9)–N(10)–B(2)	121.5(9)	Fe(1)–N(11)–N(12)	124.5(6)
N(11)–N(12)–B(2)	119.3(7)	N(2)–B(1)–N(4)	106.5(7)
N(2)–B(1)–N(6)	106.8(8)	N(2)–B(1)–C(10)	108.4(8)
N(4)–B(1)–N(6)	103.0(7)	N(4)–B(1)–C(10)	114.5(8)
N(6)–B(1)–C(10)	117.0(8)	N(8)–B(2)–N(10)	107.3(8)
N(8)–B(2)–N(12)	102.2(8)	N(8)–B(2)–C(25)	115.4(8)
N(10)–B(2)–N(12)	107.5(8)	N(10)–B(2)–C(25)	109.6(9)
N(12)–B(2)–C(25)	114.2(8)		

The change in steric energy on A_2Fe complex formation (ΔU) was assessed on the basis of the following equations:

$$Fe^{2+} + 2A^- \rightleftharpoons A_2Fe \quad (2)$$

$$\Delta U = U_{A_2Fe} - U_{Fe^{2+}} - 2U_{A^-,min} \quad (3)$$

where U_{A_2Fe} and $U_{Fe^{2+}}$ represent the steric energy of the complex and metal ion, respectively. We assumed $U_{Fe^{2+}}$ to be zero for simplicity. U_{A_2Fe} was obtained by optimizing the X-ray structure in the force field. Differences in dimensions between the optimized and X-ray structures were less than 4% with a few exceptions. The ΔU values are listed in Table 7; ΔU(LS) is the value for low-spin complexes, and ΔU(HS) is the value for high-spin complexes.

Discussion

Ligand Field Strength and Electron Density on the Nitrogen Donor Atom. Complexes **1** and **2** are usually low-spin complexes in $CHCl_3$, whereas **4** and **5** assume a high-spin state. Compound **3** is intermediate between the two groups and undergoes spin crossover around room temperature. The ligand field strength of poly(pyrazolyl)borates increases, therefore, in

(14) Sohrin, Y.; Matsui, M.; Hata, Y.; Hasegawa, H.; Kokusen, H. *Inorg. Chem.* **1994**, *33*, 4376–4383.
(15) Lopez, C.; Claramunt, R. M.; Sanz, D.; Foces, C. F.; Cano, F. H.; Faure, R.; Cayon, E.; Elguero, J. *Inorg. Chim. Acta* **1990**, *176*, 195–204.

Table 6. Mean Dimensions (Å or deg) of Chelate Rings in $[B(pz)_4]_2Fe$ (**1**), $[PhB(pz)_3]_2Fe$ (**2**), $[HB(pz)_3]_2Fe$ (**3**), and $[HB(3,5\text{-}Me_2pz)_3]_2Fe$ (**4**)

	1	**2**	**3**[a]	**4**[a]
Fe−N(2)	1.97(2)	1.97(9)	1.97(1)	2.17(2)
N(1)−N(2)	1.37(1)	1.37(2)	1.36[b]	1.38(1)
N(1)−B	1.54(1)	1.56(2)	1.54(1)	1.54(1)
N(2)···N(2)	2.75(1)	2.73(1)	2.75(1)	2.98(2)
Fe···B	3.09(1)	3.15(9)	3.08(1)	3.18(1)
N(2)−Fe−N(2)	88.5(0.6)	87.9(3.8)	88.3(0.2)	86.6(0.4)
Fe−N(2)−N(1)	120.3(0.9)	120.5(2.9)	119.9(0.4)	116.6(0.6)
N(2)−N(1)−B	117.4(1.9)	119.1(1.8)	117.9(0.4)	119.7(0.4)
N(1)−B−N(1)	107.8(1.0)	105.6(2.1)	107.6(0.7)	109.9(0.8)

[a] Data taken from ref 7. [b] Pyrazolyl rings were treated as rigid groups.

Chart 1

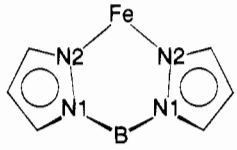

the order $[HB(3,4,5\text{-}Me_3pz)_3]^-$, $[HB(3,5\text{-}Me_2pz)_3]^-$ < $[HB(pz)_3]^-$ < $[B(pz)_4]^-$, $[PhB(pz)_3]^-$.

We have determined the acid dissociation constants of some of poly(pyrazolyl)borates in aqueous solution.[14,16] The acid dissociation constants were defined as

$$K_{a1} = [H^+][A^-]/[HA] \quad (4)$$

$$K_{a2} = [H^+][HA]/[H_2A^+] \quad (5)$$

where brackets represent the molar concentration in aqueous solution. For $[HB(3,5\text{-}Me_2pz)_3]^-$, pK_{a1} and pK_{a2} were 10.12 ± 0.05 and 5.58 ± 0.10, respectively. For $[HB(pz)_3]^-$, pK_{a1} was 6.92 ± 0.04 and pK_{a2} was 3.64 ± 0.10; for $[B(pz)_4]^-$, pK_{a1} was 6.06 ± 0.05 and pK_{a2} was 3.04 ± 0.10. These results suggest that the electron density on the nitrogen donor atom should increase in the order of $[B(pz)_4]^-$ < $[HB(pz)_3]^-$ < $[HB(3,5\text{-}Me_2pz)_3]^-$. This order is mainly dominated by inductive effect. However, it is apparent that the increasing orders of ligand field strength and of the electron density are totally reversed. Thus, the electronic effect is not the primary factor controlling the spin state of the Fe(II) complexes.

Structure of Fe(II) Poly(pyrazolyl)borate Complexes. Complexes **1**−**4** essentially have the same geometry. Poly(pyrazolyl)borates act as tripodal tridentate ligands, and the geometry about the Fe(II) atom is a trigonally distorted octahedron. The ^1H NMR spectra recorded for **1** and **2** in $CDCl_3$ indicated that their structures in solution are similar to that of the X-ray results. This is probably also true of **3** and **4**. Complexes **1**−**3** are low-spin in the crystals. Packing force probably contributes to the low-spin state of **3** in the crystal. The mean dimensions of chelate rings for **1** and **3** are identical (Table 6; the numbering scheme is shown in Chart 1). Although the dimensions of **2** are almost the same as those of **1** and **3**, complex **2** shows large variations in values of Fe−N(2), N(2)−Fe−N(2), Fe−N(2)−N(1), and N(1)−B−N(1) compared with **1** and **3**. For example, one Fe−N(2) in **2** is 2.102 Å, which is a very long bond for low-spin Fe(II). Hence, complex **2** has a more distorted octahedral geometry. This distortion is caused by intraligand contact between the phenyl and pyrazolyl groups bonded to the boron atom. The intraligand contact restricts the free conformation change of the ligand, and the nitrogen donor atoms cannot take an ideal octahedral position. This intraligand contact should be the factor that makes the low-spin state advantageous. The crystal radii of Fe(II) are 75 pm for the low-spin $^1A_{1g}$ state and 92 pm for the high-spin $^5T_{2g}$ state.[17] When coordinating a large high-spin Fe(II), poly(pyrazolyl)borates open the tripod of coordinating pyrazolyl groups. Actually, the bite size (N(2)···N(2) distance) of high-spin **4** is 0.23 Å larger than that of low-spin **1** and **3**. The opening of the tripod is realized through increasing the N(2)−N(1)−B and N(1)−B−N(1) angles. However, such a transformation is hard for $[PhB(pz)_3]^-$, since it causes severe intraligand contact. The formation of a high-spin complex is also disadvantageous for **1**, in which there is intraligand contact between the fourth and coordinated pyrazolyl rings. The bite size of 2.98 Å is quite large for $[B(pz)_4]^-$, judging from the fact that the average bite sizes of tridentate $[B(pz)_4]^-$ in reported complexes are less than 3.0 Å[18] with the sole exception of $[B(pz)_4]_2Cd$.[19] Gas-phase photoelectron spectra indicated a more pronounced trigonal distortion of high-spin **1** with respect to high-spin **3**.[6]

Figure 3 shows space-filling views of the X-ray structures of **2** and **4**. In complex **4**, the coordination around the Fe(II) atom is crowded by 3-Me groups. The mean interligand distance between 3-Me groups (Me···Me) is only 3.74 Å. When **4** forms a low-spin complex of which the dimensions are equal to those of **3**, the Me···Me distance would become 3.68 Å. This Me···Me distance is very short compared with the van der Waals radius of the methyl group (2.0 Å).[20] Therefore, interligand contact between the 3-Me groups is significantly enhanced in the low-spin complex. The interligand contact should hinder **4** from taking the low-spin state. The structure of high-spin **4** shows a large deviation of the N(2)−Fe−N(2) and Fe−N(2)−N(1) angles from 90 and 120°, respectively (Table 6). This deviation and the long Fe−N(2) distance lead to a poor overlap in the Fe−N bond. The low-spin state is more desirable for a good overlap in the Fe−N bond than the high-spin state, judging from the structure of **3**. However, **4** takes the high-spin state, since the conformation for the low-spin state is severely prohibited on account of the interligand contact.

Molecular Mechanics Calculations. Table 7 summarizes the steric energy change (ΔU) accompanying low- and high-spin complex formation. Absolute values of ΔU contain intrinsic deviations derived from used parameter sets and are not so chemically meaningful. A comparison of ΔU can be useful, however, between analogous compounds. Here, we noted the steric energy difference between the low- and high-

Table 7. Steric Energy Change (kcal/mol) for Complex Formation

compd	ΔU(LS)	ΔU(HS)	$\Delta(\Delta U)$
$[B(pz)_4]_2Fe$	75.2	71.8	3.4
$[PhB(pz)_3]_2Fe$	80.5	77.6	2.9
$[HB(pz)_3]_2Fe$	75.7	70.5	5.2
$[HB(3,5\text{-}Me_2pz)_3]_2Fe$	87.3	73.8	13.5
$[Fe(Hpz)_6]^{2+}$	91.0	77.4	13.6
$[Fe(phen)_3]^{2+}$	−5.2	−10.2	5.0
$[Fe(2\text{-}Cl(phen))_3]^{2+}$	−2.5	−14.8	12.3
$[Fe(py)_6]^{2+}$	29.7	−5.4	35.1

(16) Sohrin, Y.; Kokusen, H.; Kihara, S.; Matsui, M.; Kushi, Y.; Shiro, M. *J. Am. Chem. Soc.* **1993**, *115*, 4128−4136.

(17) Shannon, R. D. *Acta Crystallogr., Sect. A* **1976**, *32*, 751−767.

(18) (a) Restivo, R. J.; Ferguson, G.; O'Sullivan, D. J.; Lalor, F. J. *Inorg. Chem.* **1975**, *14*, 3046−3052. (b) De Gil, E. R.; Rivera, A. V.; Noguera, H. *Acta Crystallogr., Sect. B* **1977**, *33*, 2653−2655. (c) Cocivera, M.; Desmond, T. J.; Ferguson, G.; Kaitner, B.; Lalor, F. J.; O'Sullivan, D. J. *Organometallics* **1982**, *1*, 1125−1132. (d) Cocivera, M.; Ferguson, G.; Kaitner, B.; Lalor, F. J.; O'Sullivan, D. J.; Parvez, M.; Ruhl, B. *Organometallics* **1982**, *1*, 1132−1139.

(19) Reger, D. L.; Mason, S. S.; Rheingold, A. L.; Ostrander, R. L. *Inorg. Chem.* **1993**, *32*, 5216−5222.

(20) Bondi, A. *J. Phys. Chem.* **1964**, *68*, 441−451.

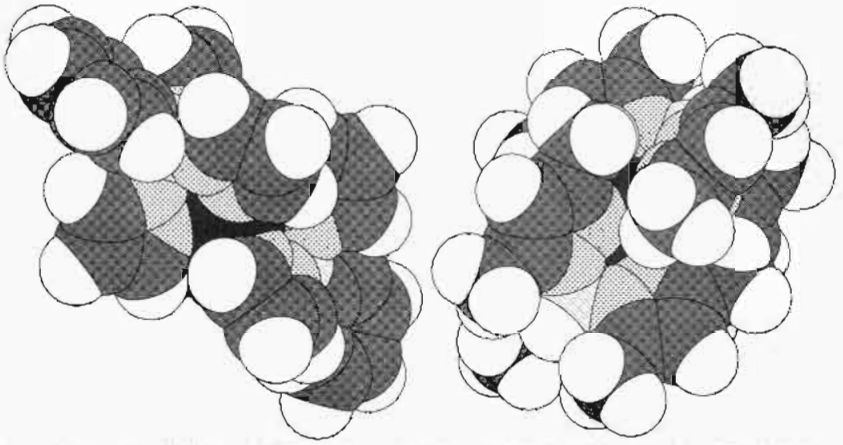

Figure 3. Space-filling views of low-spin $[PhB(pz)_3]_2Fe$ (**2**, left) and high-spin $[HB(3,5\text{-}Me_2pz)_3]_2Fe$ (**4**, right). X-ray structural data of **4** were taken from ref 7.

spin complexes:

$$\Delta(\Delta U) = \Delta U(\text{LS}) - \Delta U(\text{HS}) \quad (6)$$

We also calculated the mechanics of imaginary $[Fe(Hpz)_6]^{2+}$ for comparison. Pyrazole, of which the donor atom is sp^2-hybridized nitrogen, is probably located at a higher position in a spectrochemical series and tends to form a low-spin complex.[21] However, forming a low-spin complex is sterically disadvantageous, since the six pyrazole ligands cause interligand contact. Such contact is reflected in the large $\Delta(\Delta U)$ of 13.6 kcal/mol. In $[HB(pz)_3]^-$, the pyrazolyl groups are nicely preorganized[22] for tripodal coordination. The increase in strain energy is small when the free ligand is taken from its lower strain energy state and coordinated to a metal ion. Furthermore, when an A_2Fe type complex is formed, both ligands adopt a mutually staggered conformation, which results in only a small increase in the interligand contact. Such steric efficiency[23] favors the formation of the six-coordinate complex with a small metal ion. The $\Delta(\Delta U)$ is 5.2 kcal/mol for **3**. It is probably balanced by a favorable enthalpy gain for low-spin complex formation at ambient temperature, and **3** shows spin crossover in CH_2Cl_2. $[B(pz)_4]^-$ and $[PhB(pz)_3]^-$ destabilize the high-spin state because of the intraligand contact. The steric energy barrier, $\Delta(\Delta U)$, becomes smaller for **1** and **2** than for **3**, and the low-spin state precedes the high-spin state. On the other hand, the $\Delta(\Delta U)$ of **4** is much larger than that of **3** and comparable to that of $[Fe(Hpz)_6]^{2+}$. The interligand contact caused by the 3-Me groups cancels the steric efficiency of poly(pyrazolyl)borates for a small ion.

To confirm the validity of the above discussion, similar MM calculations were performed on $[Fe(phen)_3]^{2+}$ and $[Fe(2\text{-}Cl\text{-}phen)_3]^{2+}$ complexes (phen = phenanthroline). While $[Fe(phen)_3]^{2+}$ is low-spin, $[Fe(2\text{-}Cl\text{-}phen)_3]^{2+}$ is high-spin owing to interligand contact derived from the 2-Cl group.[24] The reported X-ray structure of $[Fe(phen)_3]^{2+}$ was used to model the initial conformations for the calculation.[24a] The steric energy was also calculated for imaginary $[Fe(py)_6]^{2+}$ (py = pyridine). Although the deviation in ΔU of these complexes was substantially different from that of the poly(pyrazolyl)borate complexes, the $\Delta(\Delta U)$ was comparable (Table 5). $\Delta(\Delta U)$ was 35.1 kcal/mol for $[Fe(py)_6]^{2+}$. The interligand contact is enhanced by the two proton atoms on the 2-position of pyridine. The interligand contact is largely relieved for the bidentate ligand phen, and $\Delta(\Delta U)$ is 5.0 kcal/mol for $[Fe(phen)_3]^{2+}$, favoring the formation of a low-spin complex. The $\Delta(\Delta U)$ is again increased for $[Fe(2\text{-}Cl\text{-}phen)_3]^{2+}$ (12.3 kcal/mol), suggesting that the interligand contact is highly unfavorable for the low-spin state.

The ligand field strength is inherently affected by the intra- and interligand contact. Hancock et al. have demonstrated this using N-donor macrocyclic ligands.[23,25] These ligands have high ligand field strength in contrast with chelating ligands. This is because the secondary nitrogen donors of the macrocycle are highly basic because of the inductive effect and the increase in steric energy is small in complex formation. Although the *N*-methyl group should enhance the basicity of the nitrogen, the ligand field strength is not increased. For example, the ligand field-splitting parameter (Δ) of Ni(II) complexes drops from 2043 cm^{-1} in the cyclam complex to 1700 cm^{-1} in the tetra-*N*-methylcyclam complex (cyclam = 1,4,8,11-tetraazacyclotetradecane).[26] MM calculations have proven that *N*-methyl groups interfere with each other to cause Ni−N bond stretching.[23,25] This decreases overlap in the bond, thus diminishing the value of Δ.

Intra- and Interligand Contact in the Chemistry of Poly(pyrazolyl)borates. In other papers, we reported the complexation of group 2 metal ions with poly(pyrazolyl)borates.[14,16] Tris- and tetrakis(pyrazolyl)borates formed octahedral A_2M complexes with group 2 metals, of which the stability was highly dependent upon the ligand. The stability of $[HB(pz)_3]^-$ complexes decreased in the order of $Mg^{2+} > Ca^{2+}$. $[B(pz)_4]^-$ readily formed a complex with Mg^{2+} but not with Ca^{2+}. The stability of $[HB(3,5\text{-}Me_2pz)_3]^-$ complexes was higher for Ca^{2+} than for Mg^{2+}. These facts were explained by the steric effects. The bite size was 2.94 Å in $[HB(pz)_3]_2Mg$ and 3.11 Å in $[HB(pz)_3]_2Ca$. Because $[HB(pz)_3]^-$ can take both bite sizes without high steric strain, it forms stable complexes with Mg^{2+} and Ca^{2+}. It is difficult for $[B(pz)_4]^-$ to open the bite size to 3.1 Å owing to the intraligand contact. The interligand contact is enhanced

(21) (a) Cotton, F. A.; Wilkinson, G. *Advanced Inorganic Chemistry*, 4th ed.; John Wiley & Sons: New York, 1980. (b) Huheey, J. E.; Keiter, E. A.; Keiter R. L. *Inorganic Chemistry*, 4th ed.; Harper Collins College Publishers: New York, 1983.
(22) Cram, D. J.; Kaneda, T.; Helgeson, R. C.; Brown, S. B.; Knobler, C. B.; Maverick, E.; Trueblood, K. N. *J. Am. Chem. Soc.* **1985**, *107*, 3645−3657.
(23) (a) Hancock, R. D.; Martell, A. E. *Chem. Rev.* **1989**, *89*, 1875−1914. (b) Hancock, R. D. *Prog. Inorg. Chem.* **1989**, *37*, 187−291.
(24) (a) Zalkin, A.; Templeton, D. H.; Ueki, T. *Inorg. Chem.* **1973**, *12*, 1641−1646. (b) Reiff, W. M.; Long, G. J. *Inorg. Chem.* **1974**, *13*, 2150−2153.
(25) Hancock, R. D.; Dobson, S. M.; Evers, A.; Ngwenya, M. P.; Wade, P. W.; Boeyens, J. C. A.; Wainwright, K. P. *J. Am. Chem. Soc.* **1988**, *110*, 2788−2794.
(26) (a) Fabbrizzi, L. *J. Chem. Soc., Dalton Trans.* **1979**, 1857−1861. (b) Herron, N.; Moore, P. *Inorg. Chim. Acta* **1983**, *36*, 117.

in $[HB(3,5\text{-}Me_2pz)_3]_2Mg$ and destabilizes the complex. Hence, the intra- and interligand contact causes a drastic change in complex stability for group 2 metal ions having a closed-shell electron configuration.

For transition and posttransition metal ions, the electron configuration can be changed by intra- and interligand contact of poly(pyrazolyl)borates. One example is the Fe(II) complexes discussed here. Reger et al. have reported that the structure and electron configuration of the Pb(II) complexes depend on substituents.[27] While $[HB(pz)_3]_2Pb$ and $[B(pz)_4]_2Pb$ contain a stereochemically active lone pair, $[HB(3,5\text{-}Me_2pz)_3]_2Pb$ takes a trigonally distorted octahedral configuration, where the lone pair is stereochemically inactive. The 3-Me groups sterically hinder the localization of the lone pair. Another example is molybdenum complexes with poly(pyrazolyl)borates, which do not obey the 18-electron rule.[28] The intra- and interligand contact contributes to the unusual electron configurations of molybdenum.

In conclusion, intra- and interligand contact is the essential factor producing the unique chemistry of poly(pyrazolyl)borates.

Acknowledgment. We are grateful to Professor Y. Hata (Kyoto University) for helpful discussions. This research was supported by Grant-in-Aid No. 06740558 from the Ministry of Education, Science and Culture of Japan.

Supporting Information Available: Tables of crystallographic details, complete positional and thermal parameters, temperature factors, bond distances, and bond angles for **1** and **2** (32 pages). Ordering information is given on any current masthead page.

IC950189T

(27) Reger, D. L.; Huff, M. F.; Rheingold, A. L.; Haggerty, B. S. *J. Am. Chem. Soc.* **1992**, *114*, 579−584.

(28) (a) Cotton, F. A.; Frenz, B. A.; Murillo, C. A. *J. Am. Chem. Soc.* **1975**, *97*, 2118−2122. (b) Skagestad, V.; Tilset, M. *J. Am. Chem. Soc.* **1993**, *115*, 5077−5083. (c) Protasiewicz, J. D.; Theopold, K. H. *J. Am. Chem. Soc.* **1993**, *115*, 5559−5569.